International Journal of Scientific & Engineering Research, Volume 5, Issue 4, April-2014
ISSN 2229-5518

DUAL-INPUT ZVZCS DC-DC CONVERTER COMBINING A BHB AND A FB CELL

*G.Tamilselvi **A.Kamal

*P.G Student **Head of the Department, Department of Electrical and Electronics Engineering

Sri Lakshmi Ammal Engineering College, Chennai, India.

Abstract— This Paper presents a new zero-voltage-switching (ZVS) isolated dc–dc converter which combines a boost half-bridge (BHB) cell and a full-bridge (FB) cell, so that two different type of power sources, i.e., both current fed and voltage fed, can be coupled effectively by the proposed converter for various applications, such as fuel cell and hybrid energy system. By fully using two high-frequency transformers and a shared leg of switches, number of the power devices and associated gate driver circuits can be reduced. With phase-shift control, the converter can achieve ZVS turn-on of active switches and zero-current switching (ZCS) turn-off of diodes. A 30–60 V input, 335 VDC output converter circuit is designed and simulated.

Index Terms— Boost half-bridge (BHB), dc–dc converter, dual input, phase-shift, soft switching and hybrid.

INTRODUCTION

Nowadays, clean and renewable energies including fuel cell, wind energy, photovoltaic, etc., have been widely applied to achieve environment friendly objectives [1] [2]. Because of the discontinuity of renewable sources, like wind energy and solar energy, generally, an auxiliary power supply is necessary to smooth output power and keep output voltage stable under various load conditions. Thus, an efficient combination of different energy sources, to be a hybrid renewable power conversion system, has become an interesting topic [3]. Moreover, high power solar cells or fuel cells are often faced with a need of boosting their low output voltage to a high dc-link voltage subjected to the requirements in grid-connecting applications [4]. A three-port series resonant converter operating at constant switching frequency was proposed in [5], which can achieve soft-switching and high frequency operation. After that, a modeling and control method based on this resonant multi-port converter was investigated in [6]. With a systematic approach [7], [8], an isolated single primary winding multiple input converter which combined a two-input buck converter and a fly back converter was studied in [9]. By applying a concept of dual active bridge (DAB) converter [10] [11], multiple-port bidirectional converter topologies employing multiple transformer windings were proposed in [12], where the separate windings are used for each port and the bidirectional power flow is easily controlled by a phase-shift angle and/or duty cycle [13]. Based on a current-fed half-bridge structure proposed in [14], the characteristics of triple port half-bridge were studied in [15] and [16]. As the conclusion given in [17], for the sustainable energy with a low output terminal voltage such as fuel cell, a boost-type converter is favorable for a high efficiency operation. A multi-input isolated boost dc-dc converter with multi-windings based on the flux additive concept was proposed in [18], but the reverse current block diode is connected in series with the MOSFETs on the primary side, which makes the bidirectional power flow impossible, so the auxiliary circuit for rechargeable elements is needed. In [19], a high step-up isolated converter with two input sources was investigated, and the converter utilizes the current-source type applying to both of the input power sources. To avoid the switch voltage spikes caused by the leakage inductor, an active clamping circuit is added in [20], has more no of switches, diodes and high frequency transformer.

This paper proposes a new step-up isolated dc–dc converter with dual input ports by combining a current-fed BHB cell and a voltage-fed FB cell, and the proposed converter can be used in applications such as hybrid electric vehicles, photovoltaic power generation systems, and fuel cell systems. Based on the circuit topology, the derivation process of the proposed converter is introduced. The steady-state operating principles and features are explained so as to demonstrate the merits of the converter. Design considerations on some critical parameters are studied. Finally, representative experimental results from a 600-W prototype are provided to validate the proposed concept. The salient advantages of the proposed converter can be summarized as follows:

1) Ability of dual-input connection;

2) Reduced number of power devices and their associated gate driver components;

3) ZVS turn-on of the main switches;

4) ZCS turn-off of the diodes without reverse recovery issue.

International Journal of Scientific & Engineering Research, Volume 5, Issue 4, April-2014
ISSN 2229-5518

PROPOSED SOFT-SWITCHED DC–DC CONVERTER

In order to hybridize the two inputs, i.e., Vin1 and Vin2, a BHB cell can be paralleled with an FB cell by adopting a mutual low voltage dc bus as shown in Fig. 1. Because of the similarity of the pulse width modulation pattern of BHB and FB cells, the switch legs I and II can be merged as a common bridge. Hereby, a new topology with full function but a simpler connection compared to the previous discrete cells is derived and illustrated in Fig. 2. The proposed converter consists of a current-fed port and a voltage-fed port, which provides a larger flexibility in practical applications with different type of power sources. Transformers T1 and T2which have the turn ratios as n1: n2 = 2:1 in this study are connected in a special way: the dotted terminals of the primary windings are connected in the conjunction point A, while two secondary windings are connected in series (it is also possible to connect them in parallel depending on different requirements).

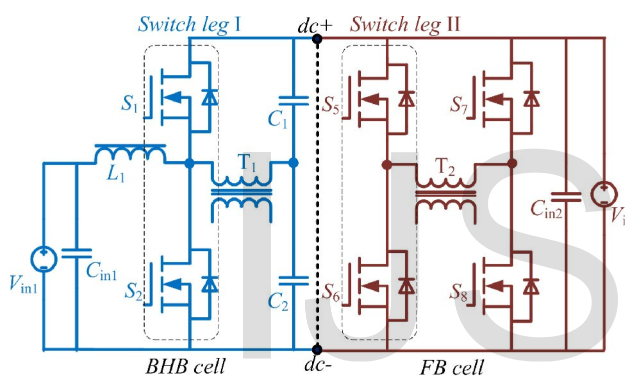

Fig. 1. Schematic of a dual-input converter with BHB and FB cells.

A voltage doubler circuit is employed on the secondary side and the voltage ringing over the diodes can inherently be clamped by the output capacitor C3 or C4 . L2 is essentially the sum of the transformer leakage inductance and an extra inductance. A dc blocking capacitor Cb is added in series with the primary winding of T2 in order to avoid transformer saturation caused by any asymmetrical operation in the FB circuit.

The proposed converter can be viewed as a voltage source vp interfaced to another voltage source vs through the energy interfacing element L2 as shown in Fig. 3. In steady state, the timing diagram and the key waveforms of the proposed converter controlled by phase-shift angle between the switch pairs, S1, S2 and S3, S4 , are presented in Fig. 4, where VL = n1 □ Vin1, VH = 12□ Vo , and Ts is the switching period. In this letter, only the symmetrical operation condition, i.e., the switching duty cycle D is 50%, is discussed, so that S1 and S2 as well as S3 and S4 have the

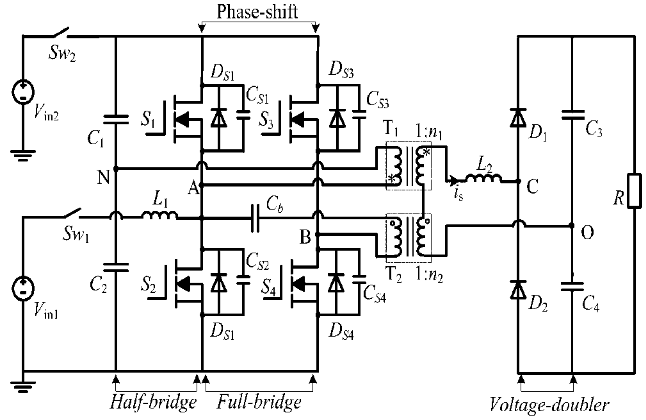

Fig. 2. Topology of the proposed hybrid dc–dc converter.

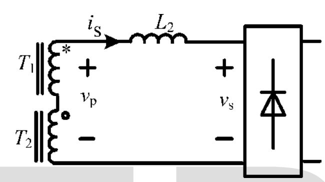

Fig. 3. Equivalent circuit of phase-shift control.

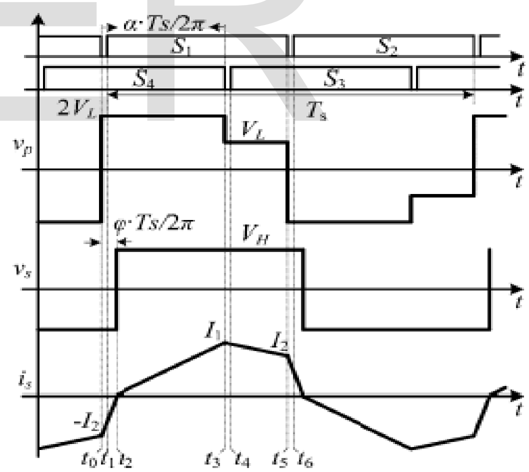

Fig. 4. Timing diagram and typical waveforms: α ≤ π

complementary driving signals that gives Vin2 = 2Vin1 . Accordingly output voltage and power transferred can only be regulated by the phase-shift angle α of the two poles of the input bridge. The power factor of the high frequency ac loop can be evaluated by the angle □ which represents the phase delay between the secondary voltage and current. In order to avoid high reactive power in the converter, the

International Journal of Scientific & Engineering Research, Volume 5, Issue 4, April-2014
ISSN 2229-5518

regulated phase-shift angle will be limited in the range: 0 ≤ α ≤ π.

Since the output diode rectifier is current driven, the following constrains must be satisfied: 1) when is is positive, vs must be positive; and 2) when is is negative, vs must be negative, and there by based on the waveforms shown in the Fig. 4(a), the operation principle of the converter can be explained as follows. During [t0, t2], as shown in Fig. 5(a), the body diodes of S1and S4conduct and Vp is clamped to a voltage of 2VL until is decreases with a slope (2VL + VH)/L2 to zero at t2. At t0, S1 turns ON under ZVS. During [t2, t3], when is becomes positive and flows through D1, S1 and S4 will conduct and is increases with a slope (2VL − VH)/L2 , as shown in Fig. 5(b). During [t3, t5], when S4turns OFF at t3, CS3 and CS4 start to resonate with L2 until VCS3 = 0, and then S3can turn ON under ZVS. Current in the primary side flows through S1 and DS3 that makes vp equal to VL ,and is decreases with a slope (VH − VL)/L2 . The equivalent circuit is given in Fig.5(c).

After t5the second half switching cycle starts. Obviously, the diodes on the secondary side will always turn OFF under ZCS in the whole operation range. From the typical waveforms in Fig. 4(a), the defined peak current values I1 and I2 are given as

$$I_1 = i_s(t_3) = \frac{2V_L - V_H}{L_2} \cdot \frac{(\alpha - \varphi)T_s}{2\pi} \quad (1)$$

$$I_2 = i_s(t_5) = \frac{2V_L + V_H}{L_2} \cdot \frac{\varphi T_s}{2\pi} \quad (2)$$

$$I_1 - I_2 = \frac{V_H - V_L}{L_2} \cdot \frac{(\pi - \alpha)T_s}{2\pi}. \quad (3)$$

To determine the value of phase delay, we can solve (3) for □ (rad)

$$\varphi = \frac{1}{4} \cdot \left(\pi + \alpha - \frac{V_H}{V_L}\pi\right). \quad (4)$$

Substituting (4) into (1) and (2), the output power of the proposed converter can be expressed

$$P_o = f(\alpha) = \begin{cases} \frac{V_H V_L}{4\omega L_2}\left(1 - \frac{V_H^2}{V_L^2}\right), & 0 \le \alpha \le \varphi \\ \frac{V_H V_L \pi \left[-3\left(\frac{\alpha}{\pi}\right)^2 + 6\left(\frac{\alpha}{\pi}\right) + \left(1 - \frac{V_H^2}{V_L^2}\right)\right]}{8\omega L_2}, & \varphi < \alpha < \pi \end{cases} \quad (5)$$

where ω represents the switching angular frequency. As a result of (5), when duty cycle and switching frequency are fixed, output power will be related to the phase-shift angle and the inductance L2 . It is worth noting that: 1) a larger L2makes the reactive power larger and the ability of power

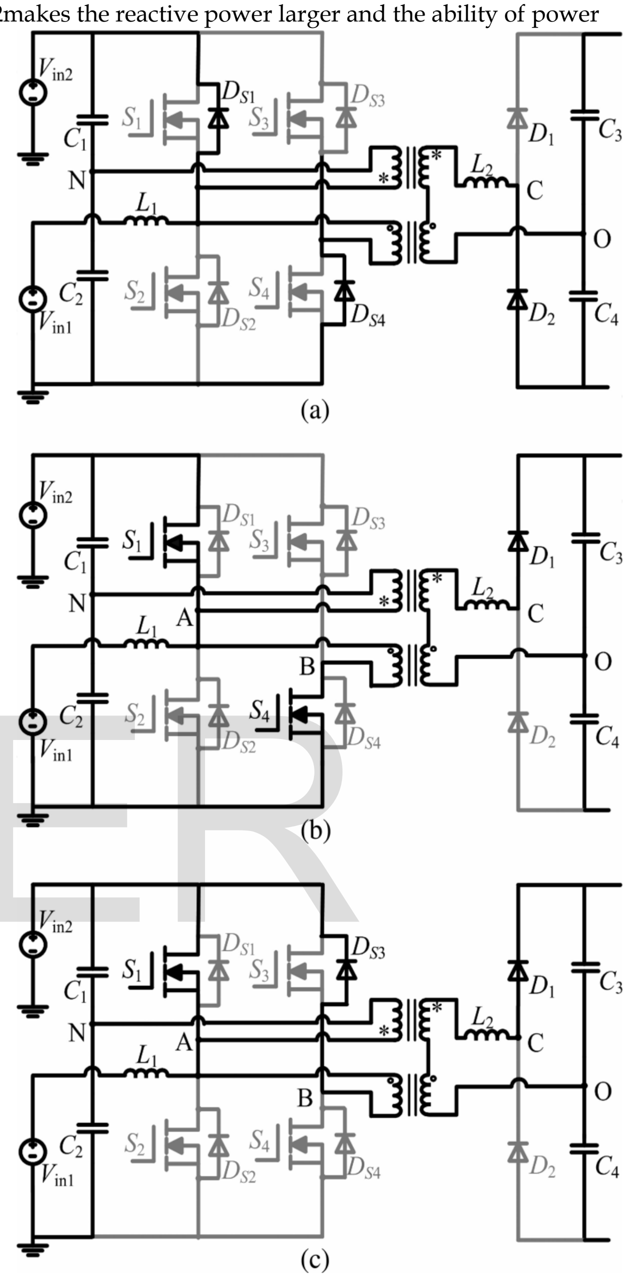

Fig. 5. Equivalent circuits of the proposed converter: (a) [t0 , t2], (b) [t2 , t3] and (c) [t3 , t5].

delivering lower; and 2) when 0 ≤ α ≤ □, the output power is approximately a constant and it depends on the

International Journal of Scientific & Engineering Research, Volume 5, Issue 4, April-2014
ISSN 2229-5518

circuit's parameters instead of α. When the inductance of L2 is small and/or the load is light, is will become discontinuous that will affect the converter's operation, so the constraints on the critical condition may be investigated from the waveforms in Fig. 6. In this case, □ is zero

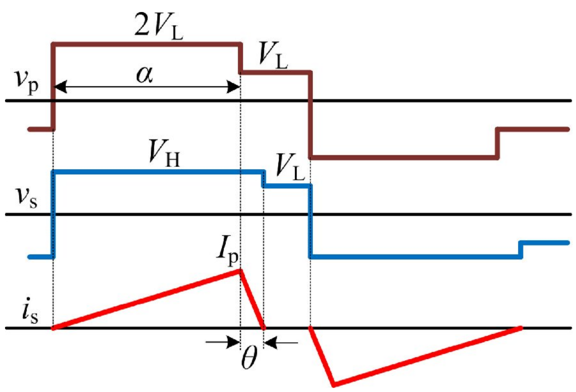

Fig.6. Typical waveforms under discontinuous is.

and the angle θ is calculated as

$$\theta = \left(\frac{V_L}{V_H - V_L} - 1 \right) \alpha. \quad (7)$$

Hence, the constraints to keep is in continuous conduction mode can be yielded

$$\theta + \alpha \geq \pi \Rightarrow \omega L_2 \geq \frac{R\alpha(\pi - \alpha)}{8(\pi + \alpha)}. \quad (8)$$

DESIGN CONSIDERATIONS

Generally, ZVS can be deduced on the precondition that the anti parallel diode of switch must conduct before the switch is triggered. In other words, the main devices are turned OFF with a positive current flowing and then the current diverts to the opposite diode which allows the in-coming MOSFET to be switched on under zero voltage. Therefore, ZVS constraints depend on the magnitude of primary side currents, i.e., (n1 + n2) □ is, iL1 and n2 □ is , and have the relationships at driving instant

$$\begin{cases} -(n_1 + n_2) \cdot i_s(t_1) - i_{L1}(t_1) < 0, & \text{for } S_1 \\ (n_1 + n_2) \cdot i_s(t_5) - i_{L1}(t_5) > 0, & \text{for } S_2 \\ n_2 \cdot i_s(t_3) > 0, & \text{for } S_3, S_4. \end{cases} \quad (9)$$

In fact, the condition of (9) for S1, S3 , and S4 can be easily satisfied, so ZVS can achieve over the whole load range and is independent on the converter's parameters. While to ensure the ZVS turn-on of S2 , the following function of the circuit parameters and the control variables must be satisfied:

$$(n_1 + n_2) I_2 \frac{V_o^2}{V_{in1} R} + \frac{V_{in1}}{2L_1 f_s} > 0 \Rightarrow \frac{(n_1 + n_2)(4n_1 + G_V)\varphi}{2\omega L_2} + \frac{1}{2L_1 f_s} > \frac{G_V^2}{R}. \quad (10)$$

Both the turn-off transient current and the rms current of S2 are approximately proportional to the phase-shift angle that means for same output power, if α decreases, switching and conduction losses of S2 will become less, so as a result the system efficiency can be improved. Regarding to this fact as well as the ZVS operation, an optimal design and tradeoff between switching loss and conduction loss may be considered for the future research.

simulation results

The proposed converter has been simulated by using MATLAB simulink. Finally, 30 to 60 V dual inputs, 335 V output is tested with 600 W power rating. Fig.7., (a), (b), (c) and (d) are the simulated output of the proposed converter.

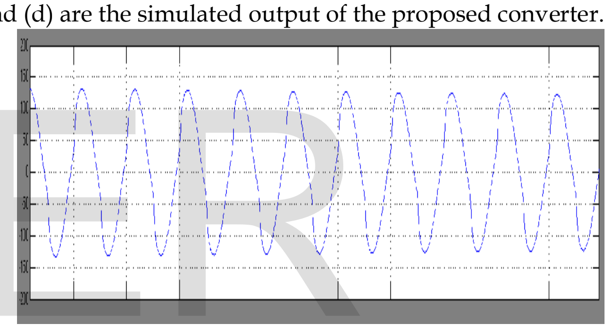

(a)

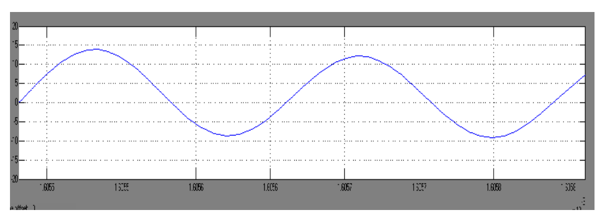

(b)

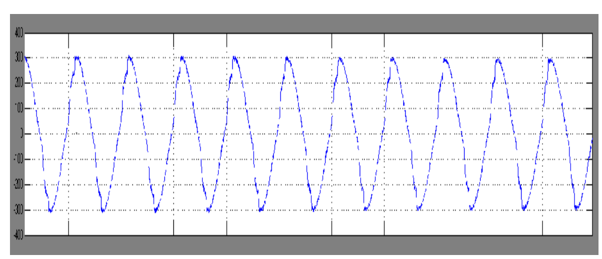

International Journal of Scientific & Engineering Research, Volume 5, Issue 4, April-2014
ISSN 2229-5518

(c)

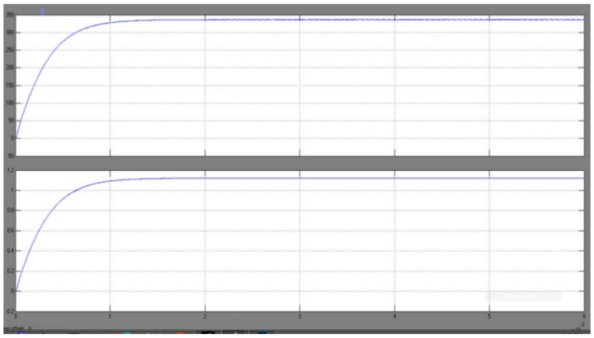

(d)

Fig. 7.(a) and (b) Transformer primary voltages 150 V and 20 V.(c)Transformer secondary voltage 300 V.(d) output voltage of the Dc-Dc converter and converter across load.

PARAMETERS AND COMPONENTS USED IN SIMULATION

Parameters	Values
Input voltages	30-50 V
Ratedoutput power	600 W
S1 and S2	SUP90N15 (150 V/90 A)
S3 and S4	SUP28N15 (150 V/28 A)
D1 and D2	15ETL06FP (600 V/15 A)
Transformers T1 and T2	1:4, 1:2, Ferrite N87
Inductors L1 and L2	20μH,KoolMμ;40 μH,n87
Switching frequency	100kHz

CONCLUSION

In this paper, a soft-switched isolated dc–dc converter with the ability of handling two independent inputs is derived, investigated, and designed. The experimental results match the theoretical analysis well. Comparing to the existing topologies, the converter proposed here has the advantages such as reduced number of power switches, higher efficiency, and simple control.

REFERENCES

[1] F. Blaabjerg, Z. Chen and S. B. Kjaer, "Power electronics as efficient interface in dispersed power generation systems,"IEEE Trans. Power Electron. 2004, 19, (5), pp.1184-1194.

[2] Z. Chen, J. Guerrero, and F. Blaabjerg, "A review of the state of the art of power electronics for wind turbines," IEEE Trans.Power Electron., 2009, 24, (8), pp. 1859–1875.

[3] M. Bragard, N. Soltau, S. Thomas and R. W. De Doncker, "The balance of renewable sources and user demands in grids: power electronics for modular battery energy storage systems," IEEE Trans. Power Electron., 2010, 25, (12), pp. 3049–3056.

[4] H. Cha, J. Choi and P. N. Enjeti, "A three-phase current-fed DC/DC converter with active clamp for low-dc renewable energy sources," IEEE Trans. Power Electron., 2008, 23, (6), pp.2784–2793.

[5] H. Krishnaswami and N. Mohan, "Three-port series-resonant dc-dc converter to interface renewable energy sources with bidirectional load and energy storage ports," IEEE Trans. Power Electron., 2009, 24, (10), pp.2289-2297.

[6] Z. Qian, O. Abdel-Rahman, H. Al-Atrash, and I. Batarseh, "Modeling and control of three-port DC/DC converter Interface for satellite applications," IEEE Trans. Power Electron., 2010, 25, (3), pp.637-649.

[7] Y.-C. Liu and Y.-M. Chen, "A systematic approach to synthesizing multi-input DC–DC converters," IEEE Trans. Power Electron., 2009, 24, (1), pp. 116–127.

[8] Y. Li, X. Ruan, D. Yang, F. Liu and C. K. Tse, "Synthesis of multiple-input DC/DC converters," IEEE Trans. Power Electron., 2010, 25, (9), pp. 2372–2385.

[9] Q. Wang, J. Zhang, X. Ruan and K. Jin, "Isolated single primary winding multiple-input converters," IEEE Trans. Power Electron., 2011.

[10] R. W. De Doncker, D. M. Divan and M. H. Kheraluwala, "A three-phase soft-switched high-power density dc/dc converter for high power applications," IEEE Trans. Ind. Appl., 1991, 27, (1), pp. 63-67.

[11] C. Mi, H. Bai, C. Wang and S. Gargies, "Operation, design and control of dual H-bridge-based isolated bidirectional DC–DC converter," IET Power Electron., 2008, 1, (4), pp. 507-517.

[12] H. Tao; A. Kotsopoulos, J.L. Duarte, M.A.M. Hendrix, "Transformer-coupled multiport ZVS bidirectional DC–DC

International Journal of Scientific & Engineering Research, Volume 5, Issue 4, April-2014
ISSN 2229-5518

converter with wide input range," IEEE Trans. on Power Electron., 2008, 23, (2), pp.771-781.

[13] C. Zhao, S. D. Round, J. W. Kolar, "An isolated three-port bidirectional DC-DC converter with decoupled power flow management," IEEE Trans. Power Electron., 2008,23,
(5), pp. 2443-2453.

[14] F. Z. Peng, H. Li, G. J. Su and J. S. Lawler, "A new ZVS bi-directional dc-dc converter for fuel cell and battery applications,"IEEE Trans. Power Electron.,2004, 19, (1), pp. 54-65.

[15] D. Liu and H. Li, "A ZVS bi-directional DC–DC converter for multiple energy storage elements," IEEE Trans. Power Electron., 2006, 21, (5), pp. 1513-1517.

[16] H. Tao, J. L. Duarte and M. A. M. Hendrix, "Three-port triple-half-bridge bidirectional converter with zero-voltage switching," IEEE Trans. Power Electron., 2008, 23, (2), pp. 782–792.

[17] M. Nymand, R. Tranberg, M. E. Madsen, U. K. Madawala, M. A. E. Andersen, "What is the best converter for low voltage fuel cell applications- A buck or boost," Proc. Annual Conference of the IEEE Industrial Electronics Society, 2009, pp. 959-964.

[18] Y.-M. Chen, Y.-C. Liu, and F.-Y. Wu, "Multi-Input DC/DC converter based on the multi winding transformer for renewable energy applications," IEEE Trans. on Ind. Appl. 2002, 38, (4), pp. 1096-1104.

[19] R. Wai, C. Lin and Y. Chang, "High step-up bidirectional isolated converter with two input power sources," IEEE Trans. Ind. Electron., 2009, 56, (7), pp.2679-2641.

[20] Z. Zhang, O. C. Thomsen, M. A. E. Andersen, and H. R. Nielsen, "Dual input isolated full-bridge boost DC-DC converter based on the distributed transformers," IET Power Electron., vol. 5, no. 7, pp. 1074–1083,Aug.2012.

1.